Astron. Astrophys. 193, 119–124 (1988)

ASTRONOMY AND ASTROPHYSICS

A hydrodynamic code for the treatment of late-type stellar wind flows based on the method of characteristics

M. Cuntz and P. Ulmschneider

Institut für Theoretische Astrophysik, Im Neuenheimer Feld 561, D-6900 Heidelberg, Federal Republic of Germany

Received July 7, accepted August 24, 1987

Summary. We describe a time-dependent eulerian hydrodynamic code based on the method of characteristics which allows the computation of radiating stellar wind flows in tube-like structures on late-type stars. The treatment of boundaries under sub- and supersonic conditions is discussed as is the introduction of shock waves into the atmosphere. Ionization is taken into account. For test and application we study the behaviour to approach limiting shock strength.

Key words: hydrodynamics – numerical methods – shock waves – stars: atmospheres of – stars: mass loss – the Sun: corona of

1. Introduction

For the investigation of stellar wind flows along coronal loops or from coronal hole regions on late-type stars it is necessary to adopt time-dependent methods. There are several reasons for this. First radiation damping, ionization and population densities strongly change with the wave amplitudes behind shocks. Second it has long been recognized that momentum transfer by waves (wave-pressure) is difficult to include in a time-independent treatment (McWhirter et al., 1975). Third nonlinear interaction and overtaking of shocks create situations which can not be described by time-independent means. For the numerical solution of the hydrodynamic equations we have chosen the characteristics method. This method allows an accurate treatment of the shock discontinuity which in finite difference and FCT methods is smeared because of artificial viscosity or diffusivity. As the radiation losses are usually strongly peaked behind the shock, the present method therefore improves the shock treatment considerably. In addition in the characteristics method it is easy to treat large numbers of shocks (we typically have 50 shocks in our test cases). Finally the characteristics method is ideally suited for the new massive parallel computers as here each height point is treated independently of its neighbours.

Time-dependent computations of stellar wind flows have been made by Klein et al. (1976) as well as Kneer and Nakagawa (1976), and Wood (1979). These authors have used finite difference methods. Innes et al. (1987) have taken a second order Godunov technique for their radiative shock calculations. Computations in coronal loops have been made by Nagai (1980), Wu et al. (1981), McClymont and Canfield (1983) using the finite difference method, and by Mariska et al. (1982) with the FCT method. The characteristics method has been used by Ulmschneider et al. (1977) and Nakagawa et al. (1987). For a more detailed review of time-dependent (magneto-)hydrodynamic wave propagation in stellar atmospheres see Ulmschneider and Muchmore (1986) and of numerical methods see Falle (1986).

Compared to the lagrangian hydrodynamic method of Ulmschneider et al. (1977, 1987) the present eulerian code had to be completely revised as now three characteristics have to be treated explicitly. In addition the lagrangian description suffers from well known difficulties when rapid mass motions are considered. First high speed wind flows in the outer layers of an atmospheric slab leads to a wide separation of individual mass points on an eulerian height scale. This results in a loss of resolution in the lagrangian computation of the outer layers. Second at the lower boundary of the lagrangian code the waves are usually introduced by specifying the gas velocity at a piston. Such a piston represents a mass element and in high speed flows a lagrangian boundary would migrate through the atmosphere necessitating a time- and space dependent specification of physical boundary values. In almost all cases such a specification can not be made. Third at the outer boundaries lagrangian codes estimate conditions as a function of time at a fixed fluid element. To avoid migration and to permit the treatment of supersonic out- and inflow this boundary condition has to be strongly modified as well. The description of our eulerian code is given in Sect. 2 while in Sect. 3 we discuss the boundary conditions. Results are presented in Sect. 4. Section 5 gives our conclusions.

2. Method of computation

In this section we describe the one-dimensional eulerian radiation hydrodynamic code for high speed flows in tube-like structures in late-type stars. We neglect radiation pressure as well as viscosity and thermal conductivity but include shocks, assuming that the shock thickness is much smaller than the usual grid spacing. Shocks in our approximation thus can be treated as discontinuities.

2.1. Treatment of regular points

Between discontinuities the gas can be described by the usual hydrodynamic equations (e.g. Landau Lifshitz, 1959)

Send offprint requests to: P. Ulmschneider

$$\frac{\partial \rho}{\partial t}+\frac{\partial \rho u}{\partial r}+\rho u \frac{1}{A} \frac{dA}{dr}=0, \tag{1}$$

$$\rho\left(\frac{\partial u}{\partial t}+u \frac{\partial u}{\partial r}\right)+\frac{\partial p}{\partial r}+\rho g(r)=0, \tag{2}$$

$$\frac{\partial S}{\partial t}+u \frac{\partial S}{\partial r}=\left.\frac{dS}{dt}\right|_{\mathrm{rad}}, \tag{3}$$

where as functions of radius r, ρ is the density, u the gas velocity, A the area of the tube, p the pressure, $g(r)$ is the gravity, S the entropy, and t is the time. $dS/dt|_{\mathrm{rad}}$ is the radiative damping function. For spherical stellar wind flows $1/A\ dA/dr = 2/r$ and

$$g(r)=g_0 \frac{r_0^2}{r^2}, \tag{4}$$

where g_0 is the gravity at the inner shell radius r_0. Considering an ionizing gas we have in addition equations relating the thermodynamic variables

$$d\rho=\left(\frac{\partial \rho}{\partial p}\right)_S dp+\left(\frac{\partial \rho}{\partial S}\right)_p dS, \tag{5}$$

$$dT=\left(\frac{\partial T}{\partial p}\right)_S dp+\left(\frac{\partial T}{\partial S}\right)_p dS, \tag{6}$$

where T is the temperature. We consider the physical state to be described by the variables u, T and p. The sound speed

$$c^2=\left(\frac{\partial p}{\partial \rho}\right)_S, \tag{7}$$

and the other thermodynamic derivatives are assumed to be given as functions of p and T. For the computation of these quantities we use the procedure described by Wolf (1983, 1985). From Eq. (5) we have

$$\frac{d\rho}{dt}=\frac{1}{c^2} \frac{dp}{dt}+\left(\frac{\partial \rho}{\partial S}\right)_p \left.\frac{dS}{dt}\right|_{\mathrm{rad}}, \tag{8}$$

with the total derivative given by

$$\frac{d}{dt}=\frac{\partial}{\partial t}+u \frac{\partial}{\partial r}. \tag{9}$$

From Eqs. (1) and (6) we thus find

$$\frac{\partial p}{\partial t}+u \frac{\partial p}{\partial r}+c^2\left(\frac{\partial \rho}{\partial S}\right)_p \left.\frac{dS}{dt}\right|_{\mathrm{rad}}+\rho c^2 \frac{\partial u}{\partial r}+\rho c^2 u \frac{1}{A} \frac{dA}{dr}=0, \tag{10}$$

$$\frac{\partial T}{\partial t}+u \frac{\partial T}{\partial r}-\left(\frac{\partial T}{\partial p}\right)_S\left(\frac{\partial p}{\partial t}+u \frac{\partial p}{\partial r}\right)-\left(\frac{\partial T}{\partial S}\right)_p \left.\frac{dS}{dt}\right|_{\mathrm{rad}}=0. \tag{11}$$

Equations (2), (10) and (11) are solved with the method of characteristics. From a linear combination of these equations the following set of characteristic equations can be derived:

$$du+\frac{1}{\rho c} dp-\rho c\left(\frac{\partial T}{\partial p}\right)_S \left.\frac{dS}{dt}\right|_{\mathrm{rad}} dt+c u \frac{1}{A} \frac{dA}{dr} dt+g(r)\, dt=0, \tag{12}$$

along the C^+ characteristic given by

$$\frac{dr}{dt}=u+c, \tag{13}$$

$$du-\frac{1}{\rho c} dp+\rho c\left(\frac{\partial T}{\partial p}\right)_S \left.\frac{dS}{dt}\right|_{\mathrm{rad}} dt-c u \frac{1}{A} \frac{dA}{dr} dt+g(r)\, dt=0, \tag{14}$$

along the C^- characteristic given by

$$\frac{dr}{dt}=u-c, \tag{15}$$

and

$$dT-\left(\frac{\partial T}{\partial p}\right)_S dp-\left(\frac{\partial T}{\partial S}\right)_p \left.\frac{dS}{dt}\right|_{\mathrm{rad}} dt=0, \tag{16}$$

along the fluid path characteristic C^0 given by

$$\frac{dr}{dt}=u. \tag{17}$$

Here we have used the thermodynamic relation

$$\left(\frac{\partial \rho}{\partial S}\right)_p=-\rho^2\left(\frac{\partial T}{\partial p}\right)_S. \tag{18}$$

2.2. Radiation loss

For the radiative losses various methods can be used with grey or non-grey non-LTE H^- continuum and Ca II, Mg II line emission (Schmitz et al., 1985; Ulmschneider and Muchmore, 1986; Ulmschneider et al., 1987) and non-LTE hydrogen $Ly\alpha$ and Ly continuum emission (Ulmschneider and Carlsson, 1988; in preparation). In outer stellar atmospheres a simple radiation loss formula developed in the thin plasma approximation is often used (McWhirter et al., 1975; Rosner et al., 1978; Athay, 1981, 1986).

$$\left.\frac{dS}{dt}\right|_{\mathrm{rad}}=-\frac{\Phi_{\mathrm{rad}}}{\rho T}=-\frac{n_e n_H}{\rho T} P_{\mathrm{rad}}(T), \tag{19}$$

where Φ_{rad} is the net radiative cooling rate (erg cm^{-3} s^{-1}). For Φ_{rad} we have chosen the Cox and Tucker type radiation law $n_e n_H P_{\mathrm{rad}}(T)$ where $P_{\mathrm{rad}}(T)$ is a function of temperature fitted to computed radiation losses in the solar model of Vernazza et al. (1973), n_e is the electron, n_H the hydrogen number density. As compared to the other radiation loss formulae the RHS of Eq. (19) does not provide radiative heating. Thus if shock heating were missing in our calculation the cooling would lead to unphysically low temperatures.

2.3. Treatment of shocks

In our code the hydrodynamic shocks are treated as discontinuities. This is valid if the molecular mean free path is much smaller than the typical size of the mesh used in the computation. The radiation region around the shocks which usually is much larger than the molecular mean free path is not treated as discontinuity but is always resolved to ensure the correct treatment of the energy balance. For the general computational treatment of the shock we follow Ulmschneider (1977, Fig. 19). As the presence of ionization and the Euler frame produce complications we give here a more detailed discussion of our shock treatment.

In addition to the four compatibility relations (along the C^+, C^-, C^0 characteristics) in front of the shock and along the C^+ characteristic behind the shock there are three Rankine–Hugoniot relations to determine the seven unknowns at the shock. These unknowns are the pressures p_1, p_2, temperatures T_1, T_2 and velocities u_1, u_2 at the pre- and postshock points and the shock speed U_{sh}. The Rankine–Hugoniot conditions are given by (Landau Lifshitz, 1959)

$$\rho_1 v_1 = \rho_2 v_2, \tag{20}$$

$$p_1 + \rho_1 v_1^2 = p_2 + \rho_2 v_2^2, \tag{21}$$

$$E_1 + \frac{p_1}{\rho_1} + \frac{1}{2} v_1^2 = E_2 + \frac{p_2}{\rho_2} + \frac{1}{2} v_2^2, \tag{22}$$

where E_1, E_2 are the internal energies and v_1, v_2 are flow speeds relative to the shock given by

$$v_1 = u_1 - U_{\rm sh}, \tag{23}$$

$$v_2 = u_2 - U_{\rm sh}. \tag{24}$$

For the numerical procedure to compute the unknowns at the shock we derive from Eqs. (20) to (24) the following relations

$$E_2 - E_1 - \frac{1}{2}(p_1 + p_2)\left(\frac{1}{\rho_1} - \frac{1}{\rho_2}\right) = 0, \tag{25}$$

$$p_1 + \rho_1 (u_1 - U_{\rm sh})^2 - p_2 - \rho_2 (u_2 - U_{\rm sh})^2 = 0, \tag{26}$$

$$U_{\rm sh} = \frac{\rho_2 u_2 - \rho_1 u_1}{\rho_2 - \rho_1}. \tag{27}$$

With estimates of all variables we compute the shock position and the preshock values u_1, p_1, T_1 at the new time using the three characteristics in front of the shock. With the original estimate of u_2 and $U_{\rm sh}$ and the updated preshock values we then solve Eqs. (25) and (26) together with the thermodynamic relations $\rho_2(p_2, T_2)$ and $E_2(p_2, T_2)$ using a Newton–Raphson scheme on the variables p_2, T_2, ρ_2 and E_2. After every cycle of that scheme we update $U_{\rm sh}$ using Eq. (27). The postshock C^+ characteristic is subsequently used to update u_2, after which the whole sequence is repeated to convergence. The internal energy, the density and the many thermodynamic derivatives needed for this procedure are computed using the method described by Wolf (1983, 1985).

3. Boundary conditions

In this section we describe the boundary conditions used in our time-dependent calculations. As discussed above the eulerian code and the introduction of shocks at the lower boundary require a modified boundary treatment in comparison with that used in a lagrangian code.

3.1. Inner boundary condition

Figure 1 shows the run of the characteristics for the different possible situations at the inner boundary. Solid characteristics emanate from known and dashed from unknown physical states at the old time level. For the physical state at the new time level one condition can be derived by solving an ordinary differential equation along each solid characteristic. As conditions along the dashed characteristics cannot be computed they have to be replaced by more or less arbitrary boundary conditions. The state is completely described when the three quantities, the gas velocity u and the two thermodynamic variables p and T are specified.

Let us consider the boundary conditions for incoming shock waves. Following the usage of our lagrangian calculations we specify the gas velocity. For linear sawtooth waves if w_0 is a steady wind velocity, u_0 a given velocity amplitude and P the

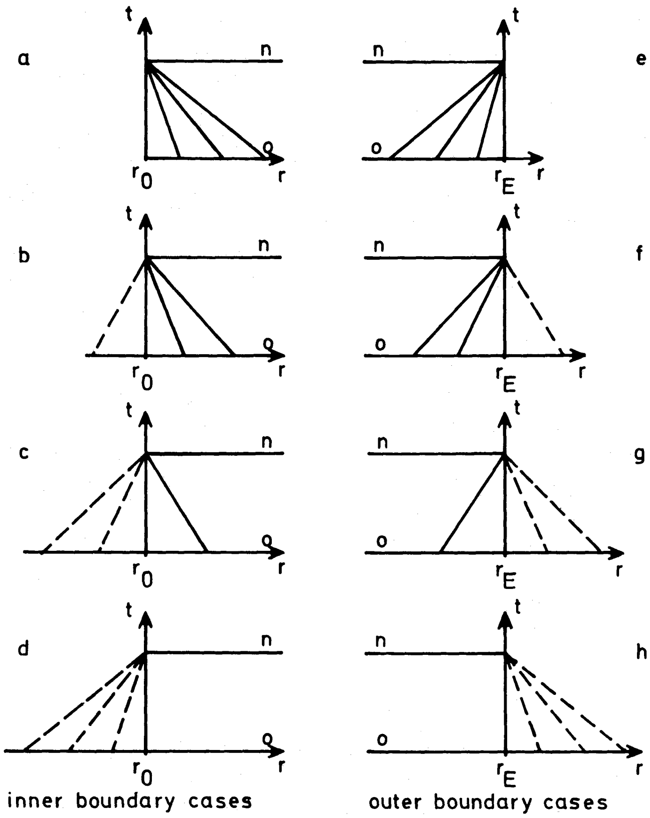

Fig. 1. Time-space plots of characteristics for the inner and outer boundary cases of an atmospheric shell extending from radius r_0 to radius r_E. The symbols o and n label old and new time levels. Dashed characteristics are not available

wave period we have

$$u(r_0, t) = -2\frac{\Delta t}{P} u_0 + w_0, \qquad 0 \le \Delta t \le \frac{P}{2}, \tag{28}$$

$$u(r_0, t) = 2\left(1 - \frac{\Delta t}{P}\right) u_0 + w_0, \qquad \frac{P}{2} \le \Delta t < P, \tag{29}$$

where

$$\Delta t = t - P \text{ entier } (t/P). \tag{30}$$

In the time interval $0 \le \Delta t < P/2$ and if $w_0 = 0$ the fluid path C^0 characteristic exists (cf. Fig. 1b, *subsonic outflow*) and the missing variables can be calculated by solving the corresponding equations along the C^0 and the C^+ characteristic.

But for $P/2 < \Delta t < P$ the fluid path is outside the known region (Fig. 1c, *subsonic inflow*). Here an additional quantity must be specified. As shock wave calculations (e.g. Ulmschneider et al., 1978, Fig. 2) show that the thermodynamic quantities also have a sawtooth profile we assume that when the density cannot be computed it behaves as

$$\rho(r_0, t) = -2\frac{\Delta t}{P} \Delta\rho_0 + \bar{\rho}(r_0), \qquad 0 \le \Delta t \le \frac{P}{2}, \tag{31}$$

$$\rho(r_0, t) = 2\left(1 - \frac{\Delta t}{P}\right) \Delta\rho_0 + \bar{\rho}(r_0), \qquad \frac{P}{2} \le \Delta t < P, \tag{32}$$

where $\bar{\rho}$ is an arbitrary mean density. At the moment $\Delta t = P/2$ where the shock enters the boundary the preshock state can be computed. The postshock values are derived from the preshock state and the known postshock velocity by solving the Rankine–Hugoniot relations using the procedure described in Sect. 2.3. Thus the postshock density at the shock is known and $\Delta\rho_0$ can be calculated using an estimate of $\bar{\rho}$ and Eq. (32). For cases where the density is a linear saw tooth $\bar{\rho}$ is the mean density at the boundary point. In practice $\bar{\rho}$ can be found from shock waves which have completely entered the atmosphere or as average of the density jump at the shock. In cases of appreciable wind with subsonic speed we use Eq. (31). If we have the case $w_0 > u_0$ the density must be completely specified.

In case of *supersonic inflow* (Fig. 1d) three characteristics have to be replaced by boundary conditions because all three characteristics emanate from the unknown region. Here in addition to the velocity two thermodynamic quantities must be specified. The case of *supersonic outflow* (Fig. 1a) does not need boundary conditions as here all characteristics emanate from known physical states. In this case the boundary point can be computed as an interior point.

3.2. *Outer boundary condition*

Except in some trivial cases in which the problem of time-dependent dynamical flows can be solved analytically, we do not know the behaviour of the gas velocity and the thermodynamic quantities at the outer boundary. Hence the boundary conditions for the outgoing waves have to be discussed explicitly. As opposed to a lagrangian boundary an eulerian boundary does not represent a fixed mass element. Here the C° characteristic which indicates the fluid path must be taken into account. Depending on the relation between the flow speed and the local sound speed we have to distinguish four different cases. These are: sub- and supersonic inflow and sub- and supersonic outflow.

For *subsonic outflows* (cf. Fig. 1f) we use a transmitting boundary condition which extrapolates the flow velocity along the C^+ characteristic (Ulmschneider et al., 1977; see also Ulmschneider, 1986). The compatibility relations along the C^+ and C^0 characteristics which emanate from the known region then allow to compute the remaining two unknowns, the pressure and temperature at the new time level. In the case of *subsonic inflow* (Fig. 1g) the foot point of the fluid path is not contained in the known region. Here we extrapolate the physical variables across the boundary to obtain the foot point of the C^0 characteristic. The procedure is then the same as for the subsonic outflow case.

For cases of *supersonic outflow* (cf. Fig. 1e) all characteristics needed for describing the physical state at the new time level emanate from the known region. Boundary conditions can not be used here because the physical variables are determined as for an interior point. In the case of *supersonic inflow* (Fig. 1h), however, all three characteristics come from outside the known region. In most cases of physical interest one has no information on the time-dependent behaviour of the flow speed and the thermodynamic quantities in the overlying region. In our numerical scheme we extrapolate here all physical variables across the boundary in the old time level and derive the physical state at the boundary point in the new time level as if all characteristics were given.

4. Results and discussion

In this section we describe results from test calculations which have been made to show on the one hand the validity of the code and on the other to demonstrate why time-dependent (as opposed to time-independent) computations are necessary if one wants to understand the complicated relation between flow and heating in outer stellar atmospheres. For our computations we selected a stellar model appropriate for Arcturus (α Boo) for which we assume the following stellar parameters, radius $R_* = 26\,R_\odot$ (Johnson et al., 1977; Augason et al., 1980), surface gravity $g_* = 50\ \mathrm{cm\,s^{-2}}$ (Martin, 1977; Ayres and Johnson, 1977), and effective temperature $T_{\mathrm{eff}} = 4250$ K (Johnson et al., 1977). An important property of shocks in isothermal gravitational atmospheres derived from weak shock theory is that the shocks have the tendency to attain a *limiting shock strength* (Osterbrock, 1961; Ulmschneider, 1970). This property explains the almost constant strength of shocks in atmospheric wave calculations (Ulmschneider et al., 1977, 1978). We want to demonstrate this behaviour with our code.

4.1. *Limiting shock strength behaviour in an idealized isothermal atmosphere*

We consider a plane parallel isothermal atmospheric layer with temperature $T_0 = 4000$ K which extends by about $4.5\,10^{11}$ cm. An initial static model was computed assuming hydrostatic equilibrium, a mean molecular weight appropriate for a neutral medium, and a pressure of $10^2\ \mathrm{dyn\,cm^{-2}}$ at the inner boundary point. We reduce the gravity to $5\ \mathrm{cm\,sec^{-2}}$ corresponding to an inner shell radius of $3.16\,R_*$. This value was chosen to ensure that we have weak shocks. Figure 2 shows typical adiabatic

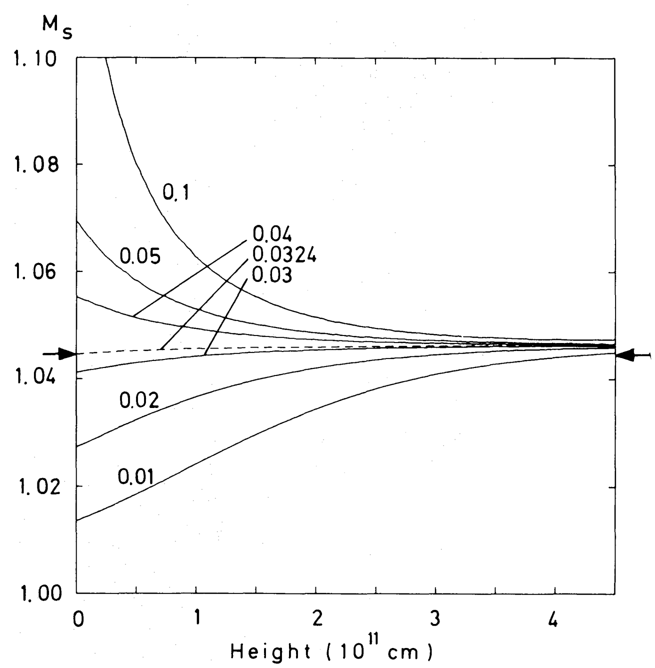

Fig. 2. Approach of the shock strength M_s to a limiting shock strength for a series of acoustic waves of different energy and fixed period $P = 1.4\,10^4$ s in an isothermal gravitational atmosphere. The theoretical limiting shock strength $M_s^{\lim}$ after Eq. (34) is indicated by arrows. The values indicate initial flow Mach numbers M_0

acoustic wave calculations where linear sawtooth shocks were introduced at the inner boundary as given by Eqs. (28) to (32). The waves have different initial flow Mach numbers $M_0 = u_0/c_0$ and a period of $P = 1.4\ 10^4$ s which is 1/10 of the acoustic cut-off period at the top of the convection zone (Ulmschneider et al., 1979; Bohn, 1984). It is readily seen in Fig. 2 that the shock Mach number M_s of the waves shows a limiting behaviour. The shock Mach number is defined as

$$M_s = \frac{U_{sh} - u_1}{c_1} \tag{33}$$

where U_{sh} is the shock speed, u_1 and c_1 the gas and sound velocity, respectively, in front of the shock. Note that in the atmosphere shown in Fig. 2 there are roughly 50 shocks. The run of M_s versus radius is obtained by time-averaging.

This limiting behaviour of M_s is explained as the balance between the two opposing effects of steepening of the wave due to energy conservation in an atmosphere with a density gradient and shock dissipation. In waves with high energy the dissipation (amplitude decay) dominates, while in those of low energy amplitude growth prevails. This limiting shock strength behaviour is well known from time-independent work (Osterbrock, 1961; Ulmschneider, 1970). Recently Hartmann and McGregor (1980), Böhm-Vitense (1986) and Hammer (1987) have argued on basis of such analytic shock strength properties, the latter two authors to gain considerable insight in the behaviour of the chromosphere-corona interface. For the limiting shock strength one finds for an non-ionizing, isothermal, plane parallel atmosphere of sound speed c_0 under the assumptions of constant g and γ

$$M_s^{\lim} = 1 + \frac{\gamma g}{4c_0} P, \tag{34}$$

valid for adiabatic calculations in the limit of $M_s \to 0$ (Ulmschneider, 1970). Figure 2 shows that the predicted value is closely reached, demonstrating the accuracy of our numerical scheme.

4.2. *Limiting shock strength behaviour in a realistic atmosphere*

Figure 3 using the stellar data of α Boo shows a series of wave calculations of period $1.4\ 10^4$ s and various energies. Ionization (in LTE) of hydrogen and radiation damping are explicitly taken into account. In addition we assume a height dependent gravity and spherical symmetry. The initial atmosphere has a temperature of 4000 K. The shocks are no longer weak. Consequently the increase of the mean atmospheric temperature due to different wave heating also enters the calculations. The curves are labelled in terms of the initial velocity amplitude given by the Mach number M_0. It is interesting that the property of the wave amplitude to reach a common limiting shock strength is still retained. The strong decrease of the wave amplitudes in the most energetic waves is primarily caused by enhanced radiation damping behind the shocks.

The limiting shock strength behaviour for waves of identical initial energy but different period in a considerably extended atmosphere is shown (solid) in Fig. 4. We assume an initial amplitude of $M_0 = 0.10$ and three different wave periods. The atmosphere extends now from 1.05 R_* to 1.25 R_*. For comparison we have plotted two different versions of $M_s^{\lim}$ after Eq. (34).

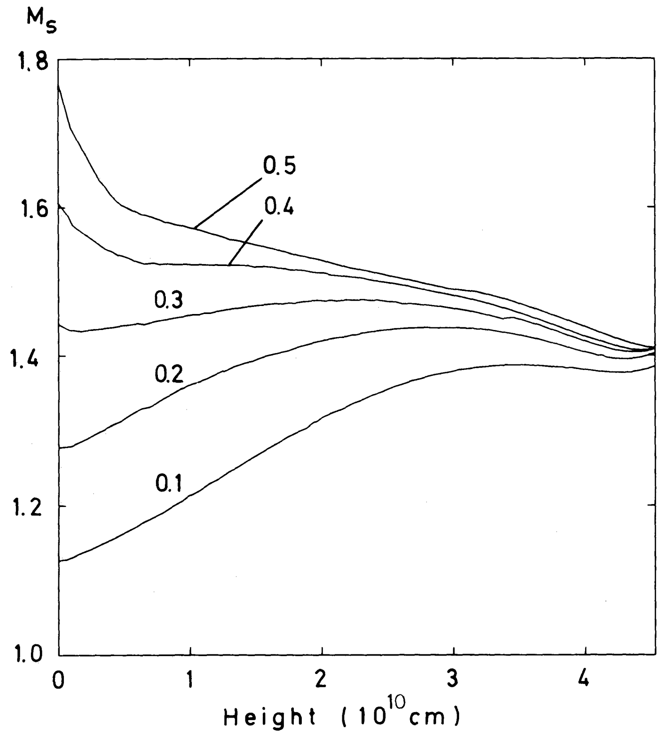

Fig. 3. Approach of the shock strength M_s to a limiting value for acoustic waves of fixed period $P = 1.4\ 10^4$ s in a spherically symmetric atmosphere model of α Boo where height dependent gravity, ionization and radiation damping are considered. The values indicate initial flow Mach numbers M_0

The dashed lines in Fig. 4 show values of $M_s^{\lim}$ assuming no ionization, $T = 6000$ K, $\gamma = 5/3$ but with a height dependent gravity. The second (dotted) version of $M_s^{\lim}$ takes $c_0 = \langle c \rangle$ and γ from the time-dependent model. It is seen that initially all wave amplitudes attempt to approach the dashed values $M_s^{\lim}$ until ionization and radiation damping leads to a rapid decrease of the amplitudes.

For short period waves the amplitude remains small and it is not surprising that the dotted values of $M_s^{\lim}$ valid for weak shocks are reached. This limit however depends on the properties of the atmosphere which suffers shock heating, ionization and radiative cooling. For waves with larger wave periods we find a rapidly increasing discrepancy between the numerical shock strength and that predicted from Eq. (34). This shows that even if c_0 and γ is given from a time-dependent model calculation the true behaviour can only very crudely be predicted from the weak shock formula.

5. Conclusions

We have shown that the method of characteristics is well suited for the computation of stellar wind flows in late-type stars. In the approximation to treat hydrodynamic shocks as discontinuities, which is valid in cases where the molecular mean free path is much smaller than the typical numerical grid size, the present method allows to handle large numbers of shocks. Radiation and ionization can be included without difficulty. The possible boundary conditions for the cases of sub- or supersonic in- and outflow have been discussed.

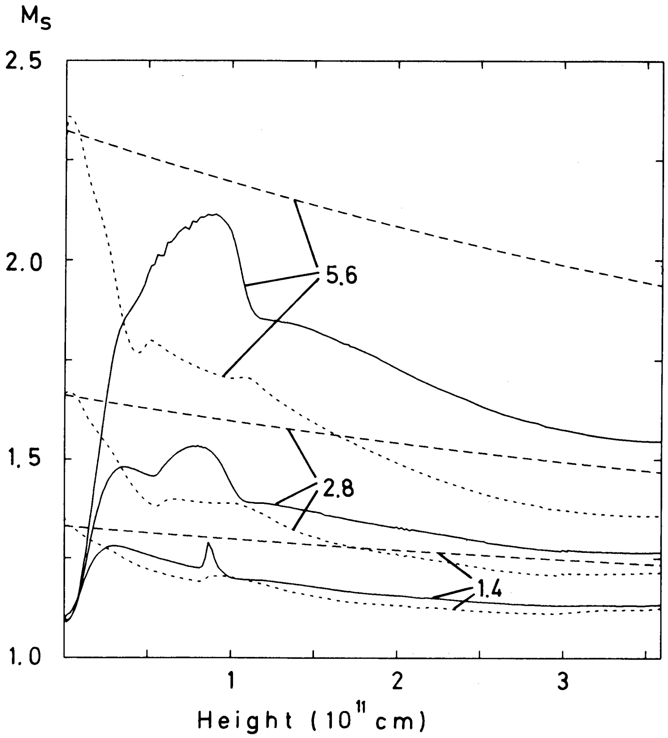

Fig. 4. Same as Fig. 3 however for a fixed initial velocity amplitude $M_0 = 0.10$ and different wave periods indicated in 10^4 s. Dashed values refer to the prediction of the limiting strength after Eq. (34) using $T = 6000$ K and $\gamma = 5/3$. Dotted values predict the limiting strength after Eq. (34) where c_0 and γ are taken from the time-dependent model

We have employed our method for monochromatic shock wave calculations in atmospheric shell models of α Boo. Here the procedure to admit shock waves at the inner shell boundary and to transmit the waves at the outer shell boundary have been discussed in detail. In a neutral, plane parallel, isothermal atmospheric slab of low gravity we have investigated whether our code reproduces the well known property of weak shocks to approach *limiting shock strength*. In this limit independently of the initial conditions a balance is reached between the dissipation related amplitude decay and the steepening influence of the atmosphere. In these tests we found that the theoretical weak shock strength limit (cf. Eq. 34) was reached with high accuracy.

As found by other authors (e.g. Ulmschneider et al., 1977) limiting shock strength is also reached in more realistic stellar wind calculations where ionization, radiation damping, shock dissipation and variable gravity is taken into account. In these applications the shock strengths do not need to be small. It was found that the limiting shock strength in these cases can not be predicted by the simple weak shock formula (Eq. 34) but can only be obtained by a time-dependent computation (cf. Fig. 4).

Acknowledgements. We gratefully acknowledge support by the Sonderforschungsbereich 132 and the Deutsche Forschungsgemeinschaft Project Ul 57/11-1.

References

Athay, R.G.: 1981, *Astrophys. J.* **250**, 709
Athay, R.G.: 1986, *Astrophys. J.* **308**, 975
Augason, G.C., Taylor, B.J., Strecker, D.W., Erickson, E.F., Wittenborn, F.C.: 1980, *Astrophys. J.* **235**, 138
Ayres, T.R., Johnson, H.R.: 1977, *Astrophys. J.* **214**, 410
Böhm-Vitense, E.: 1986, *Astrophys. J.* **301**, 297
Bohn, H.U.: 1984, *Astron. Astrophys.* **136**, 338
Falle, S.A.E.G.: 1986, in *Cosmical Gas Dynamics*, ed. F.D. Kahn, VNU Science Press, Utrecht
Hammer, R.: 1987 in *Proc. DES Inauguration Workshop, Tenerife* 1986, eds. E.H. Schröter et al., Cambridge U.P. (in press)
Hartmann, L., McGregor, K.B.: 1980, *Astrophys. J.* **242**, 260
Innes, D.E., Giddings, J.R., Falle, S.A.E.G.: 1987, *Monthly Notices Roy. Astron. Soc.* **226**, 67
Johnson, H.R., Collins, J.G., Krupp, B., Bell, R.A.: 1977, *Astrophys. J.* **212**, 760
Klein, R.I., Stein, R.F., Kalkofen, W.: 1976, *Astrophys. J.* **205**, 499
Kneer, F., Nakagawa, Y.: 1976, *Astron. Astrophys.* **47**, 65
Landau, L.D., Lifshitz, E.M.: 1959, *Fluid Mechanics*, Pergamon, London
Mariska, J.T., Boris, J.P., Oran, E.S., Young, T.R. Jr., Doschek, G.A.: 1982, *Astrophys. J.* **255**, 783
Martin, P.: 1977, *Astrophys. J.* **61**, 591
McClymont, A.N., Canfield, R.C.: 1983, *Astrophys. J.* **265**, 483
McWhirter, R.W.P., Thonemann, P.C., Wilson, R.: 1975, *Astron. Astrophys.* **40**, 63
Nagai, F.: 1980, *Solar Phys.* **68**, 351
Nakagawa, Y., Hu, Y.Q., Wu, S.T.: 1987, *Astron. Astrophys.* **179**, 354
Osterbrock, D.E.: 1961, *Astrophys. J.* **134**, 347
Rosner, R., Tucker, W.H., Vaiana, G.S.: 1978, *Astrophys. J.* **220**, 643
Schmitz, F., Ulmschneider, P., Kalkofen, W.: 1985, *Astron. Astrophys.* **148**, 217
Ulmschneider, P.: 1970, *Astron. Astrophys.* **4**, 144
Ulmschneider, P.: 1977, *Mem. Astron. Soc. Ital.* **48**, 439
Ulmschneider, P.: 1986, *Astron. Astrophys.* **168**, 308
Ulmschneider, P., Muchmore, D.: 1986, in *Small Magnetic Flux Concentration in the Solar Photosphere*, eds. W. Deinzer, M. Knölker, H.H. Voigt, Abhandl. Akad. Wissensch., Vanderhoeck und Ruprecht, Göttingen
Ulmschneider, P., Muchmore, D., Kalkofen, W.: 1987, *Astron. Astrophys.* **177**, 292
Ulmschneider, P., Nowak, T., Bohn, U.: 1977, *Astron. Astrophys.* **54**, 61
Ulmschneider, P., Schmitz, F., Hammer, R.: 1979, *Astron. Astrophys.* **74**, 229
Ulmschneider, P., Schmitz, F., Kalkofen, W., Bohn, H.U.: 1978, *Astron. Astrophys.* **70**, 487
Vernazza, J.E., Avrett, E.H., Loeser, R.: 1973, *Astrophys. J.* **184**, 605
Wolf, B.E.: 1983, *Astron. Astrophys.* **127**, 93
Wolf, B.E.: 1985, *Astron. Astrophys.* **145**, 278
Wood, P.R.: 1979, *Astrophys. J.* **227**, 220
Wu, S.T., Kan, L.C., Nakagawa, Y., Tandberg-Hanssen, E.: 1981, *Solar Phys.* **70**, 137